Denitrification losses in response to N fertiliser rates - a synthesis of high temporal resolution N2O, in-situ 15N2O and 15N2 measurements and fertiliser 15N recoveries in intensive sugarcane systems

Naoya Takeda[1], Johannes Friedl[2], Robert Kirkby[1], David Rowlings[1], Clemens Scheer[3], Daniele De Rosa[4], and Peter R Grace[1]

[1]Queensland University of Technology
[2]Queensland Institute of Technology
[3]IMK-IFU, Karlsruhe Institute of Technology
[4]European Commission, Joint Research Centre (JRC), Sustainable Resources Directorate, Land Resources Unit

December 22, 2022

Abstract

Denitrification is a key process in the global nitrogen (N) cycle, causing both nitrous oxide (N2O) and dinitrogen (N2) emissions. However, estimates of seasonal denitrification losses (N2O+N2) are scarce, reflecting methodological difficulties in measuring soil-borne N2 emissions against the high atmospheric N2 background and challenges regarding their spatio-temporal upscaling. This study investigated N2O+N2 losses in response to N fertiliser rates (0, 100, 150, 200 and 250 kg N ha-1) on two intensively managed tropical sugarcane farms in Australia, by combining automated N2O monitoring, in-situ N2 and N2O measurements using the 15N gas flux method and fertiliser 15N recoveries at harvest. Dynamic changes in the N2O/(N2O+N2) ratio (< 0.01 to 0.768) were explained by fitting generalised additive mixed models (GAMMs) with soil factors to upscale high temporal-resolution N2O data to daily N2 emissions over the season. Cumulative N2O+N2 losses ranged from 12 to 87 kg N ha-1, increasing non-linearly with increasing N fertiliser rates. Emissions of N2O+N2 accounted for 31–78% of fertiliser 15N losses and were dominated by environmentally benign N2 emissions. The contribution of denitrification to N fertiliser loss decreased with increasing N rates, suggesting increasing significance of other N loss pathways including leaching and runoff at higher N rates. This study delivers a blueprint approach to extrapolate denitrification measurements at both temporal and spatial scales, which can be applied in fertilised agroecosystems. Robust estimates of denitrification losses determined using this method will help to improve cropping system modelling approaches, advancing our understanding of the N cycle across scales.

Hosted file

952409_0_art_file_10553641_rn85fj.docx available at https://authorea.com/users/568832/articles/614545-denitrification-losses-in-response-to-n-fertiliser-rates-a-synthesis-of-high-temporal-resolution-n2o-in-situ-15n2o-and-15n2-measurements-and-fertiliser-15n-recoveries-in-intensive-sugarcane-systems

Denitrification losses in response to N fertiliser rates – a synthesis of high temporal resolution N_2O, in-situ $^{15}N_2O$ and $^{15}N_2$ measurements and fertiliser ^{15}N recoveries in intensive sugarcane systems

Naoya Takeda*[1], Johannes Friedl*[1], Robert Kirkby[1], David Rowlings[1], Clemens Scheer[1, 2], Daniele De Rosa[3], Peter Grace[1]

[1] Centre for Agriculture and the Bioeconomy, Queensland University of Technology, Brisbane, Queensland, Australia

[2] IMK-IFU, Karlsruhe Institute of Technology, Garmisch-Partenkirchen, Germany

[3] European Commission, Joint Research Centre (JRC), Sustainable Resources Directorate, Land Resources Unit, I-21027 Ispra, Italy

*Corresponding Authors: Naoya Takeda (n3.takeda@qut.edu.au), Johannes Friedl (johannes.friedl@qut.edu.au)

Key Points:

- A novel method to estimate N_2O+N_2 losses by combining high-frequency N_2O data, the in-situ ^{15}N gas flux method and fertiliser ^{15}N recoveries
- Denitrification losses in sugarcane systems were 12–87 kg N ha^{-1} mostly as N_2 (> 94%) and increased non-linearly with increasing N rates
- Denitrification accounted for 31–78% of N fertiliser losses while the proportion of reactive N losses increased with increasing N rates

Abstract

Denitrification is a key process in the global nitrogen (N) cycle, causing both nitrous oxide (N_2O) and dinitrogen (N_2) emissions. However, estimates of seasonal denitrification losses (N_2O+N_2) are scarce, reflecting methodological difficulties in measuring soil-borne N_2 emissions against the high atmospheric N_2 background and challenges regarding their spatio-temporal upscaling. This study investigated N_2O+N_2 losses in response to N fertiliser rates (0, 100, 150, 200 and 250 kg N ha^{-1}) on two intensively managed tropical sugarcane farms in Australia, by combining automated N_2O monitoring, in-situ N_2 and N_2O measurements using the ^{15}N gas flux method and fertiliser ^{15}N recoveries at harvest. Dynamic changes in the $N_2O/(N_2O+N_2)$ ratio (< 0.01 to 0.768) were explained by fitting generalised additive mixed models (GAMMs) with soil factors to upscale high temporal-resolution N_2O data to daily N_2 emissions over the season. Cumulative N_2O+N_2 losses ranged from 12 to 87 kg N ha^{-1}, increasing non-linearly with increasing N fertiliser rates. Emissions of N_2O+N_2 accounted for 31–78% of fertiliser ^{15}N losses and were dominated by environmentally benign N_2 emissions. The contribution of denitrification to N fertiliser loss decreased with increasing N rates, suggesting increasing significance of other N loss pathways including leaching and runoff at higher N rates. This study delivers a blueprint approach to extrapolate denitrification measurements at both temporal and spatial scales, which can be applied in fertilised agroecosystems. Robust estimates of denitrification losses determined using this method will help to improve cropping system modelling approaches, advancing our understanding of the N cycle across scales.

Plain Language Summary

Denitrification is a key soil process in the global nitrogen (N) cycle. Denitrification produces a potent greenhouse gas, nitrous oxide (N_2O), but also turns reactive N into environmentally benign dinitrogen (N_2). The response of these N losses to N fertiliser inputs is critical to reducing environmental impacts while maintaining crop productivity in agriculture. However, difficulties in measuring and upscaling N_2 emissions at the farm scale hinder estimation of denitrification losses, leaving denitrification as a major uncertainty for N budgets. This study quantified denitrification losses in response to N fertiliser rates on sugarcane farms in Australia, by combining automated greenhouse gas monitoring systems, N isotope techniques and statistical models. This unique approach demonstrated denitrification as a major N loss pathway, increasing nonlinearly with increasing N rates. Fertiliser N budgets showed that environmentally harmful N losses increased more than proportionally with N inputs. These findings emphasise that excessive N fertiliser use leads to agronomic inefficiency with severe adverse effects on the surrounding ecosystems such as the Great Barrier Reef. The novel approach presented here will advance our understanding of N cycling across scales and thus aid in reducing the environmental footprint of global agricultural production.

1 Introduction

Denitrification is a key process in the global nitrogen (N) cycle, reducing nitrate (NO_3^-) to gaseous N emissions in the form of nitrous oxide (N_2O) and dinitrogen (N_2). Emissions of N_2O contribute to climate change, as N_2O is a long-lived atmospheric trace gas with a global warming potential 273 times higher than that of carbon dioxide (CO_2) over a 100-year period (IPCC, 2021) and the largest remaining threat to the stratospheric ozone layer (Portmann et al., 2012; Ravishankara et al., 2009). Emissions of N_2, while environmentally benign, still represent a loss of N from the system, with potential detrimental effects on crop growth and productivity in agricultural systems. Despite a growing body of denitrification research delivering both N_2O and N_2 data from different agroecosystems, the ratio between reactive N_2O and N_2 remains a major uncertainty for N budgets across scales (Friedl et al., 2020a; Scheer et al., 2020). Growing evidence of non-linear responses of N_2O emissions to N fertiliser rates (Shcherbak et al., 2014; Takeda et al., 2021a) together with increasing fertiliser ^{15}N loss with increasing N rates (Rowlings et al., 2022; Schwenke & Haigh, 2016; Takeda et al., 2021b) in intensive cropping systems suggests excessive N inputs promote denitrification losses and lead to inefficiency of N use and adverse environmental impacts. Constraining the response of denitrification losses to N fertiliser rates is therefore critical for sustainable N management strategies to reduce N losses while maintaining crop productivity.

Yet, measuring N_2 emissions from the soil against the high atmospheric N_2 background remains challenging (Friedl et al., 2020a; Groffman et al., 2006), reflected in the small number of studies quantifying both N_2O and N_2 in the field. The Helium/Oxygen atmosphere method (He/O_2 method) (Butterbach-Bahl et al., 2002; Scholefield et al., 1997) and the ^{15}N gas flux method (Mosier & Schimel, 1993) are considered suitable for the direct quantification of N_2 and N_2O from soils. For the He/O_2 method, soil cores are incubated in the laboratory and the headspace atmosphere inside the closed incubation system is replaced with a He/O_2 mixture to measure soil-borne N_2 emissions. Field-scale seasonal/annual N_2 emissions can be estimated by repeated short laboratory measurements of soil cores, which are returned to the field after incubation. Uncertainty in the cumulative emissions with this approach however remains high due to disturbance of the soil, as in-situ measurements are not possible with this method (Chen et al., 2019; Zistl-Schlingmann et al., 2019). The ^{15}N gas flux method is the only method to measure N_2 emissions under both laboratory and field conditions. The method requires highly enriched ^{15}N fertiliser to be applied to a designated plot. Gas samples are taken using the static chamber method and analysed for their different isotopologues of N_2 and N_2O via isotope ratio mass spectrometry (IRMS) (Friedl et al., 2020a). As a result, evaluation of denitrification losses under field conditions is scarce and mostly limited to measurement periods of less than a month (Baily et al., 2012; Buchen et al., 2016; Friedl et al., 2017; Warner et al., 2019;

Weier et al., 1998), as the sensitivity of this method declines in response to the decrease of the ^{15}N enrichment in the soil NO_3^- pool. Due to the shortcomings of available direct measurement methods, estimates of cumulative denitrification losses over the crop growing season require upscaling approaches accounting for the highly dynamic response of denitrification to its drivers.

Denitrification losses have been estimated by applying the average ratio between N_2O and N_2 emissions measured for a short period under laboratory conditions to N_2O emissions measured over the crop growing season under field conditions (Scheer et al., 2009). Burchill et al. (2016) measured the N_2:N_2O ratio bimonthly in the field and interpolated the ratio linearly between sampling events to apply to more frequent N_2O measurements. However, the ratio between N_2O and N_2 is highly variable and changes rapidly in a non-linear fashion depending on interactions between environmental drivers of denitrification such as soil water content (Friedl et al., 2016), temperature (Bizimana et al., 2021), C availability (Qin et al., 2017) and N substrate availability (Chen et al., 2019; Warner et al., 2019), leading to considerable bias and large uncertainty in N_2 estimation if a fixed ratio is used. Wang et al. (2020) correlated the $N_2O/(N_2O+N_2)$ ratio measured under laboratory conditions to multiple soil factors and applied the ratio to field-measured N_2O to estimate field-scale seasonal N_2 emissions. These approaches account for the dynamic response of the N_2:N_2O ratio to key drivers. However, the absence of plants may bias the measured ratios, as plant-soil-microbe interactions are known to both affect magnitude and partitioning of N_2 and N_2O emissions (Henry et al., 2008; Malique et al., 2019). Furthermore, inevitable disturbance of soil through sampling is also of concern, while the lack of in-situ measurements hinders the direct validation of the N_2:N_2O ratio calculated as a function of key drivers. These shortcomings denote a high uncertainty of field-scale seasonal N_2 estimates using current approaches and demand a refined method that allows for robust estimates of N_2 and N_2O emissions. Critically, accounting for the dynamic responses of the ratio between N_2O and N_2 to soil factors needs to occur under field conditions in the presence of plants. Such estimates are urgently needed to constrain N budgets in different agroecosystems and to refine N fertiliser management strategies for both agronomic and environmental benefits.

The aim of this study was to estimate seasonal denitrification losses (N_2O+N_2) in response to N fertiliser rates in intensively managed tropical sugarcane (*Saccharum* spp.) systems in Australia, by combining high temporal resolution N_2O measurements with automated greenhouse gas (GHG) monitoring systems, in-situ measurements of $N_2O/(N_2O+N_2)$ ratio with the ^{15}N gas flux method and fertiliser ^{15}N recoveries. The dynamic changes in the $N_2O/(N_2O+N_2)$ ratio observed in the field were explained by fitting generalised additive mixed models (GAMMs) with soil temperature, water-filled pore space (WFPS), soil mineral N contents and CO_2 emissions, enabling spatio-temporal upscaling of high temporal frequency N_2O measurements to N_2 emissions. Fertiliser-derived N_2O+N_2 losses were further calculated and compared

with fertiliser ^{15}N loss, corroborating the estimates of N_2O+N_2 at the cumulative scale and differentiating fertiliser ^{15}N loss pathways. Establishing the response of N_2O+N_2 losses as well as their proportion of fertiliser ^{15}N loss to N fertiliser application rates with this innovative approach will refine N budget estimates across scales and allow evaluation of N fertiliser management strategies accounting for N losses from agroecosystems.

2 Materials and Methods

In this study, in-situ measurements of N_2O and N_2 emissions from two sugarcane systems were combined with previously reported high temporal resolution measurements of N_2O (Takeda et al., 2022; Takeda et al., 2021a) and recovery of ^{15}N-labelled fertiliser in the plant, soil and N_2O (Takeda et al., 2022; Takeda et al., 2021b) presented in the previous studies to quantify seasonal N_2O and N_2 losses.

2.1 Study site

The field experiments were conducted on commercial sugarcane farms in Burdekin, QLD (19° 37’ 4’’ S, 147° 20’ 4’’ E) from October 2018 to August 2019 and in Mackay, QLD (21° 14’ 4’’ S, 149° 04’ 6’’ E) from October 2019 to August 2020, described in details in Takeda et al. (2022). The climate is tropical in both Burdekin and Mackay. The soil is classified as Brown Dermosol and Brown Kandosol in the Australian Soil Classification (Isbell, 2016), or Luvisol and Fluvisol in the World Reference Base (WRB) Classification (IUSS Working Group, 2014), at the Burdekin and Mackay sites, respectively. Sugarcane varieties Q240 and Q208 were planted in 2015 and 2016 and the crop was the 3rd ratoon during the experiment at the Burdekin and Mackay sites, respectively. Irrigation was applied by furrow irrigation at the Burdekin site and overhead sprinkler at the Mackay site. Sugarcane is burnt before harvest to remove the leaves at the Burdekin site, leaving little trash (crop residues) on the ground. ‘Green cane trash blanketing (GCTB)’, a practice where the cane is harvested green and the trash is spread over the ground, is practised at the Mackay site. Selected soil physical and chemical parameters are shown in Table 1.

Table 1 Soil properties at 0-0.2 m depth at the Burdekin and Mackay sites

Variable	Burdekin	Mackay
BD (g cm^{-3})	1.3	1.1
pH (H_2O)	6.92	4.13
Total C (%)	1.60	1.35
Total N (%)	0.08	0.09
Clay (%)	35.4	22.2
Silt (%)	26.0	15.9
Sand (%)	38.7	61.9
Mineral N (kg N ha^{-1})	37.0	31.8

2.2 Experimental design

A detailed description of the experimental design and setup at the Burdekin and Mackay sites can be found in Takeda et al. (2021a) and Takeda et al. (2022), respectively. Briefly, treatments at the Burdekin site were arranged in a randomised strip design with four plots across two strips for each N treatment. The experiment at the Mackay site had a completely randomised block design with three replicates per treatment, accompanied by an unfertilised control (0N) plot with three subplots. Fertiliser N rate treatments included 0N, 150 kg N ha^{-1} (150N), 200 kg N ha^{-1} (200N) and 250 kg N ha^{-1} (250N), plus 100 kg N ha^{-1} (100N) at the Mackay site only. The recommended N application rate was based on the district yield potential and soil C content as outlined in the SIX EASY STEPS protocol of the Australian sugar industry (Schroeder et al., 2010) and was 150N at the Mackay site and 200N at the Burdekin site. Urea was applied by banding the fertiliser 10 cm deep and 30 cm from the bed centre on both sides of the cane row at the Burdekin site and by stool splitting 10 cm deep at the bed centre of the cane row at the Mackay site. For the ^{15}N recovery in the soil and the plant, a 2.0 m section was excluded from the application of unlabelled N fertiliser in each plot and ^{15}N enriched urea fertiliser (5 atom%) in solution was manually applied at the corresponding rate, matching the N fertiliser placement at the respective site.

2.3 Measurement of N_2O emissions using an automated chamber system

Soil-borne N_2O and CO_2 emissions were measured at a high temporal resolution using an automated chamber system (Grace et al., 2020) from 17 October 2018 to 15 August 2019 at the Burdekin site and from 3 October 2019 to 24 August 2020 at the Mackay site. Details of the automated chamber system are given in Supporting Information S1.1. Manual gas sampling was conducted for the control plots of the Mackay site by the static closed chamber method (Friedl et al., 2017), detailed in Supporting Information S1.2. The

placement of the chambers accounted for N fertiliser placement and irrigation practice at each site: At the Burdekin site, chambers were installed covering the area from (a) the fertiliser band to the centre of the bed (bed chamber) and (b) the fertiliser band the centre of the furrow (furrow chamber). At the Mackay site, bed chambers (a) were placed at the centre of the bed (i.e., on the fertiliser band) and furrow chamber measurements (b) were substituted with those from the control plots. Daily N_2O and CO_2 emissions were calculated by averaging the measured hourly fluxes over a 24-h period from each chamber and multiplying by 24. Missing daily N_2O and CO_2 emissions between measurements were imputed by linear interpolation.

2.4 ^{15}N-labelled N_2 and N_2O sampling and analysis in the micro plots

The application of highly enriched ^{15}N urea fertiliser enabled us to quantify N_2 and N_2O emissions and their respective ratio, as well as the contribution of N fertiliser to N_2 and N_2O emissions. Micro plots were established alongside the main plots with N fertiliser rates of 150, 200 and 250 kg N ha^{-1} at the Burdekin site and with 100, 150, 200 and 250 kg N ha^{-1} at the Mackay site. The micro plots were arranged in a completely randomised block design with four replicates. A steel base (0.22 m × 0.22 m at the Burdekin site and 0.2 m × 0.4 m at the Mackay site) was installed in each micro plot and ^{15}N enriched urea fertiliser (70 atom%) was applied inside the base at the corresponding rates. Gas sampling was conducted with static closed chambers at the Burdekin site from November 2018 to February 2019 and with semi-automated chambers at the Mackay site from October 2019 to January 2020 (Takeda et al. (2022), Supporting Information S1.3). The gas samples were analysed for the concentration of N_2O and CO_2 using a Shimadzu GC-2014 Gas Chromatograph (Shimadzu, Kyoto, Japan) and for different isotopologues of N_2 and N_2O using an Isotope Ratio Mass Spectrometer (IRMS) (20–22 Sercon Limited, UK).

2.5 The ^{15}N gas flux method

The ^{15}N enrichment of the soil NO_3^- pool undergoing denitrification (a_p) and the fraction of N_2 and N_2O emitted from this pool (f_p) were calculated following the equations outlined by Spott et al. (2006) and given in the Supporting Information S1.4. Multiplying the headspace concentrations of N_2 by the respective f_p value gave N_2 emitted via denitrification, with fluxes expressed in g N_2-N emitted ha^{-1} d^{-1}. The precision of the IRMS for N_2 based on the standard deviation of atmospheric air samples (n = 18) at 95% confidence intervals was 4.4×10^{-7} and 6.0×10^{-7} for ^{29}R ($^{29}N_2/^{28}N_2$) and ^{30}R ($^{30}N_2/^{28}N_2$), respectively. The corresponding method detection limit ranged from 0.005 g N_2-N ha^{-1} d^{-1} with a_p assumed at 50 atom % to 0.014 g N_2-N ha^{-1} d^{-1} with a_p assumed at 20 atom %. For each gas sample, the product ratio RN_2O was calculated as $N_2O/(N_2O+N_2)$.

2.6 Plant and soil sampling and analyses

Plant and soil samples were taken from each of the 2.0 m sections prior to harvest (on 27–28 August 2019 at the Burdekin site and 25–26 August 2020 at the Mackay site). The procedure of plant and soil sampling and analyses are detailed in Takeda et al. (2021b) and Takeda et al. (2022) as well as Supporting Information S1.5. Briefly, aboveground sugarcane biomass, trash on the ground, two green leaves at the 3rd node from the section and the adjacent row and remaining stools and major roots of sugarcane were harvested. Soil samples were taken at three to four points between the bed and furrow centres using a soil corer and a post-hole driver down to 1.0 m. The dried plant and soil samples were then finely ground and analysed for N and ^{15}N content via IRMS analysis (20–22 Sercon Limited, UK).

2.7 ^{15}N calculations

Fertiliser ^{15}N recovered in the plant, soil, N_2O and N_2 emissions were then calculated by ^{15}N mass balance (Friedl et al., 2017; Rowlings et al., 2016; Takeda et al., 2022) using equations detailed in the Supporting Information S1.6. Overall fertiliser ^{15}N loss was calculated by the difference between the N applied and fertiliser ^{15}N recovered in the soil and plant. The contribution of soil-derived N to plant N uptake, N_2O and N_2 emissions was calculated by the difference between total N and fertiliser ^{15}N recovered in each N pool. This contribution of soil-derived N includes residue fertiliser N from the previous seasons, N in the crop residue and other sources such as N deposition or fixation.

2.8 Auxiliary measurements

For soil NH_4^+ and NO_3^- measurements, soil samples (0–20 cm depth) were taken in each plot one day after fertilisation, every 3–7 days for the first three months and monthly thereafter. At each sampling event, soils were taken from the bed near the fertiliser band at the Burdekin site where N fertiliser was applied on both sides of the bed while from both bed and furrow at the Mackay site where N fertiliser was applied at the centre of the bed. Soil NH_4^+ and NO_3^- were extracted by adding 100 mL of 2 M KCl to 20 g of air-dried soil and shaking the solution for one hour, followed by NH_4^+ and NO_3^- content measurements using a Gallery™ Discrete Analyzer (Thermo Fisher Scientific, USA). Volumetric soil water content was measured at 10 cm depth every 30 minutes using a field-calibrated FDR soil moisture probe (EnviroSCAN, Sentek, Australia) and then averaged per day. Then, WFPS was calculated from the volumetric soil water content using the measured bulk density assumed constant during the season. Soil temperature in the surface soil layer (0-10 cm) was measured every five minutes using a PT100 probe (IMKO, Germany) and then averaged per day.

2.9 Upscaling N_2 emissions and statistical analysis

Statistical analyses and graphical presentations in this study were conducted using R statistical software version 3.5.2 (R Core Team, 2018) with a significant level set at $P < 0.05$. Gap-filling of missing daily measurements of N_2O and CO_2 emissions and soil NH_4^+ and NO_3^- contents was conducted with linear interpolation using "imputeTS" package (Moritz & Bartz-Beielstein, 2017).

Emissions of N_2 at the plot scale were calculated by fitting a statistical model trained with RN_2O observed in the micro plots and applying the predicted RN_2O to high-frequency measurements of N_2O emissions in the main plots. First, daily RN_2O measured in the micro plots at both sites were modelled per N rate using the following predictors: (i) soil temperature and WFPS measured at each site, (ii) soil NH_4^+ and NO_3^- contents measured near the band at the corresponding rate in the main plots, (iii) CO_2 emissions measured in the micro plots and (iv) site as a factor. Then, daily RN_2O in the main plots were predicted per plot for each bed and furrow position for the whole crop growing season using soil temperature, WFPS, soil NH_4^+ and NO_3^- contents and daily CO_2 emissions measured in the main plots. Daily N_2 emissions were calculated per plot for each bed and furrow position for the whole crop growing season as the product of predicted RN_2O and daily N_2O emissions measured in the main plots. Finally, N_2 emissions were upscaled to the plot scale by the area ratio bed:furrow = 1:1 at the Burdekin site and bed:furrow = 1:2 at the Mackay site. Cumulative N_2 emissions were calculated by the sum of daily upscaled N_2 emissions for each plot over the whole crop growing season.

Modelling of RN_2O and gap-filling of *Ndff* N_2 were conducted by fitting generalised additive mixed models (GAMMs), using a package "mgcv" (Wood, 2011) and detailed in Supporting Information S1.7. Briefly, GAMMs can quantify non-linear relationships without specifying the functional forms (De Rosa et al., 2020; Dorich et al., 2020), which were used to analyse RN_2O in response to soil variables and *Ndff* N_2 in response to days after fertilisation (DAF) and N rates. Furthermore, GAMMs allow the use of (i) the beta family suitable to model proportions ranging from 0 to 1 and (ii) random factors to handle repeated measurements.

Effects of the sites, N fertiliser treatments and bed/furrow positions on RN_2O and N_2 emissions as well as fertiliser-derived N_2O+N_2 in the proportion of the N fertiliser applied and the N fertiliser lost were examined by fitting generalised linear (mixed) models, using packages "lme4" (Bates et al., 2015) and "mgcv" (Wood, 2011). The beta family was specified for RN_2O and the proportions of fertiliser-derived N_2O+N_2 and the gamma family for N_2 together with chamber/plot as a random factor in the case of daily variables. To establish the response of cumulative N_2O+N_2 losses to N rates, (generalised) linear models were fitted for each site.

3 Results

3.1 Daily RN_2O and N_2 emissions

Daily RN_2O observed ranged from < 0.01 to 0.768 (Fig. 1) during ~120 DAF of the measurement period, peaking at values > 0.25 within 30 DAF at the Burdekin and within 60 DAF at the Mackay site. For the remainder of the measurement period, RN_2O stayed below 0.1. The range of observed RN_2O averaged for each N rate was 0.030–0.092 at the Burdekin site, smaller than 0.082–0.189 at the Mackay site (Table 2). Overall, the observed daily RN_2O correlated positively with the N fertiliser rates (Table 2).

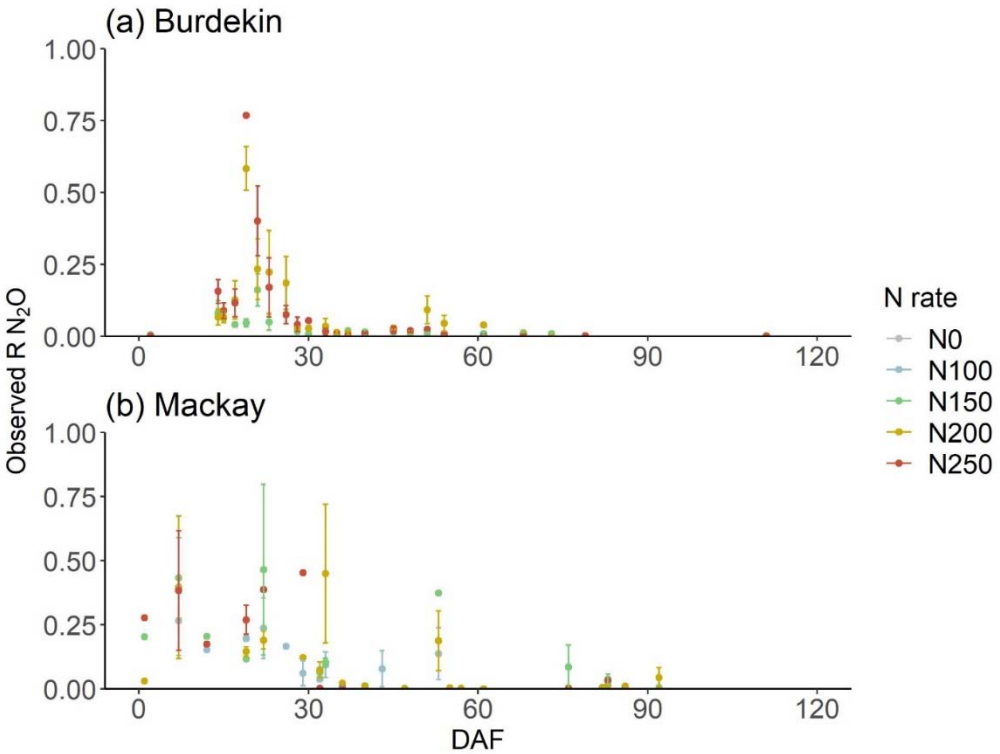

Figure 1 Observed RN_2O near the band in the micro plots over the measurement period at N rates of 100, 150, 200 and 250 kg N ha^{-1} at the Burdekin (a) and Mackay (b) sites. Points and error bars indicate mean values and standard errors

Table 2 The RN_2O observed daily, RN_2O predicted daily for bed and furrow positions and RN_2O calculated with cumulative N_2O and N_2 emissions in response to N rates ranging from 0 to 250 kg N ha^{-1}, sites and positions

Site	N rate	Observed RN_2O	Predicted RN_2O		RN_2O at cumulative
			Bed	Furrow	
Burdekin	0		0.054 ± 0.001	0.054 ± 0.001	0.024 ± 0.002
	150	0.030 ± 0.01	0.060 ± 0.002	0.061 ± 0.002	0.032 ± 0.003
	200	0.092 ± 0.02	0.061 ± 0.001	0.063 ± 0.001	0.028 ± 0.002
	250	0.072 ± 0.02	0.061 ± 0.001	0.062 ± 0.001	0.035 ± 0.001
Mackay	0		0.091 ± 0.002	0.087 ± 0.002	0.050 ± 0.001
	100	0.082 ± 0.02	0.104 ± 0.003	0.087 ± 0.002	0.048 ± 0.007
	150	0.133 ± 0.04	0.097 ± 0.002	0.086 ± 0.002	0.051 ± 0.005
	200	0.093 ± 0.03	0.115 ± 0.003	0.087 ± 0.002	0.058 ± 0.003
	250	0.189 ± 0.06	0.109 ± 0.003	0.087 ± 0.002	0.047 ± 0.007
P value					
Site		< 0.001	< 0.001		< 0.001
N rate		0.006	< 0.001		0.121
Position			< 0.001		

Fitting the RN_2O observed near the fertiliser band in the micro plots using the GAMM with Site, soil temperature, WFPS, soil NH_4^+ and NO_3^- contents and CO_2 emissions as predictors showed 51.7% of deviance explained and 0.151 of root mean square error (RMSE). The predicted RN_2O was larger at the Mackay site compared to the Burdekin site ($P < 0.001$) as well as on the bed compared to the furrow position ($P < 0.001$) (Table 2). The predicted RN_2O increased with increasing N rates ($P < 0.001$) (Table 2), which was apparent within 50 DAF (Fig. 2). The predicted RN_2O showed larger values during the late crop growing season compared to < 90 DAF (Fig. 2).

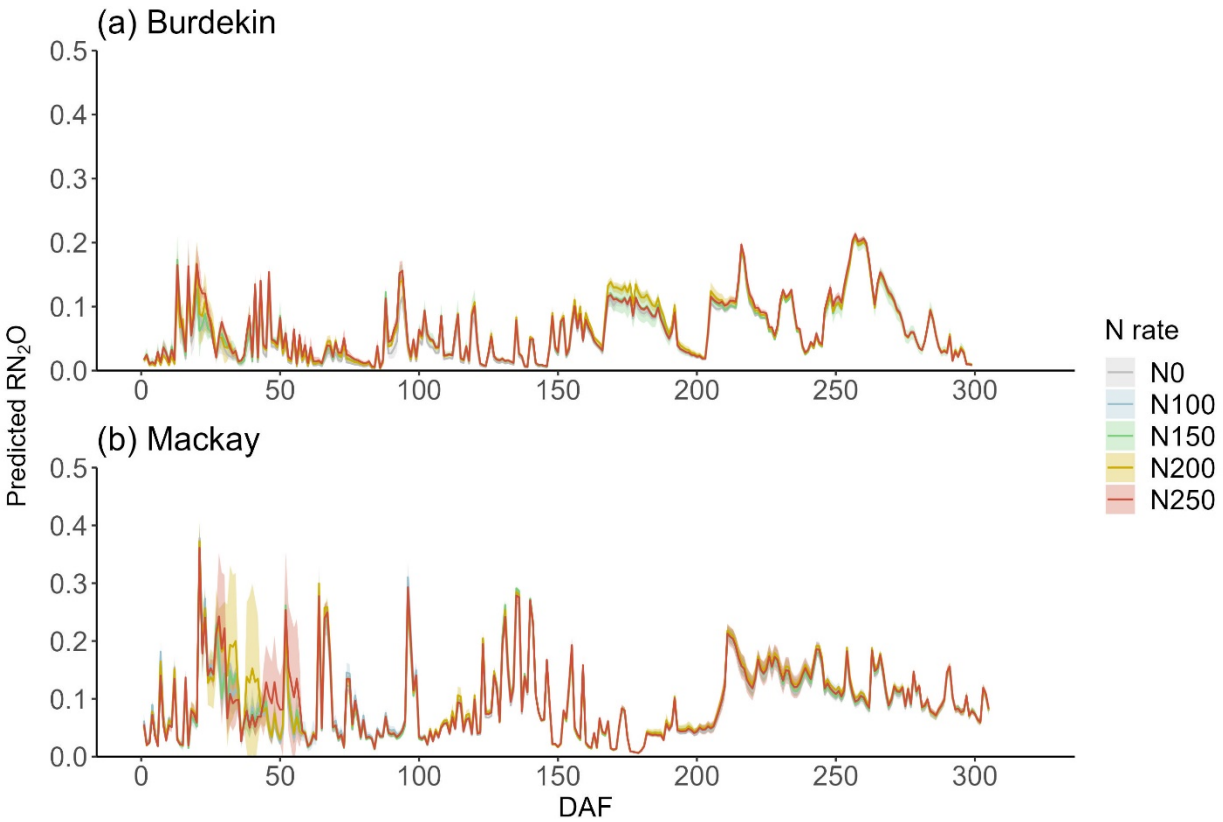

Figure 2 Daily RN_2O predicted over the crop growing season across N rates 0, 100, 150, 200 and 250 kg N ha^{-1} at the Burdekin (a) and Mackay (b) sites. Lines and shaded areas indicate predicted mean values and 95% confidence intervals

Daily N_2 emissions reached up to 5 kg N ha^{-1} d^{-1} within 50 DAF and stayed elevated for approximately 100 DAF with minor emissions for the remainder of the season (Fig. 3). Daily N_2 emissions increased with increasing N rates ($P < 0.001$) and were on average larger at the Mackay site compared to the Burdekin site ($P < 0.001$).

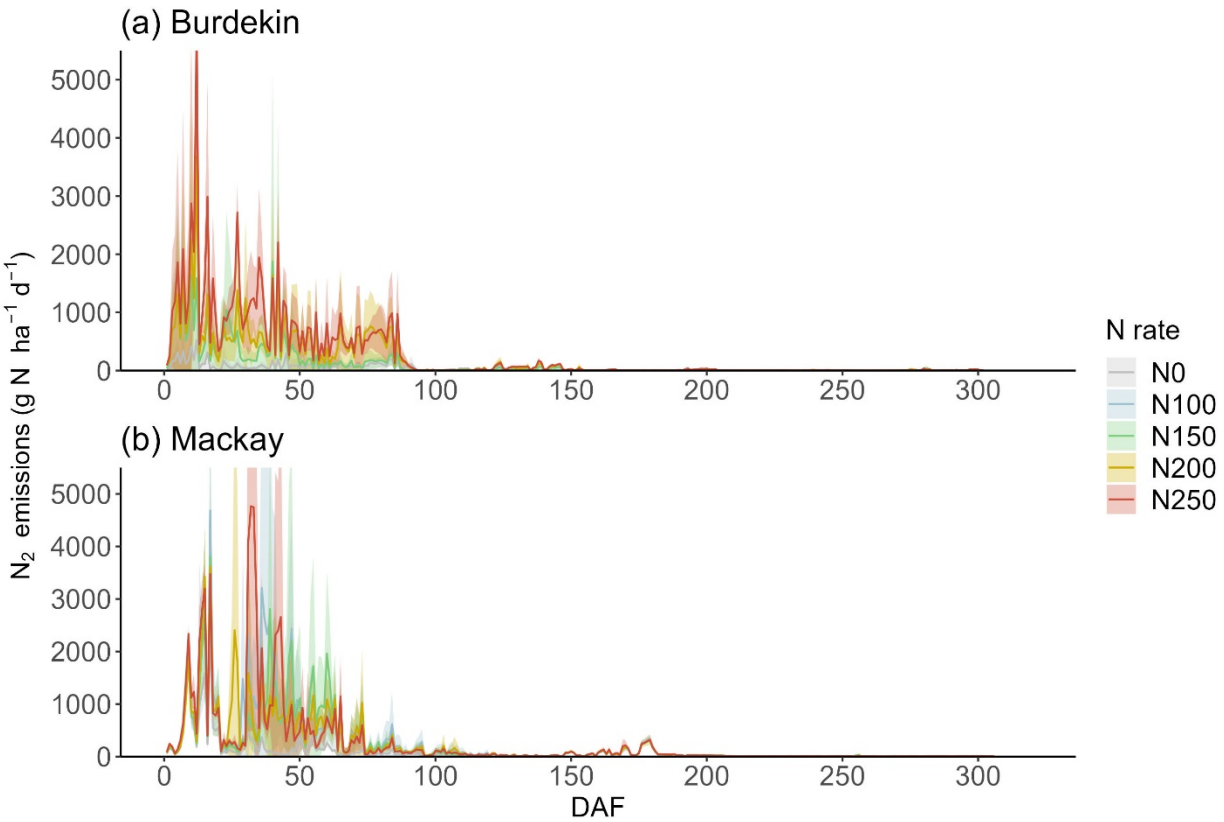

Figure 3 Daily N_2 emissions estimated over the crop growing season at N rates of 0, 100, 150, 200 and 250 kg N ha^{-1} at the Burdekin (a) and Mackay (b) sites. Lines and shaded areas indicate predicted mean values and 95% confidence intervals, respectively

3.2 Cumulative denitrification losses (N_2O+N_2)

Cumulative denitrification losses (N_2O+N_2) for the whole growing season increased exponentially from 11.9 ± 2.9 to 87.8 ± 14.4 kg N ha^{-1} with increasing N fertiliser rates from 0 to 250 kg N ha^{-1} at the Burdekin site (Fig. 4). At the Mackay site, cumulative N_2O+N_2 emissions increased from 29.5 ± 2.5 kg ha^{-1} in the unfertilised treatment to a range from 71.7 ± 5.0 to 83.2 ± 6.5 kg N ha^{-1} observed across N rates from 100-250 kg N ha^{-1}, with no differences between N fertilised treatments (Fig. 4). Overall, cumulative N_2O+N_2 emissions were larger at the Mackay site compared to the Burdekin site ($P = 0.027$). Cumulative emissions of N_2O accounted for 2.4–3.5% of N_2O+N_2 emissions at the Burdekin site, which was lower than 4.8–5.8% at the Mackay site ($P < 0.001$) (Table 2).

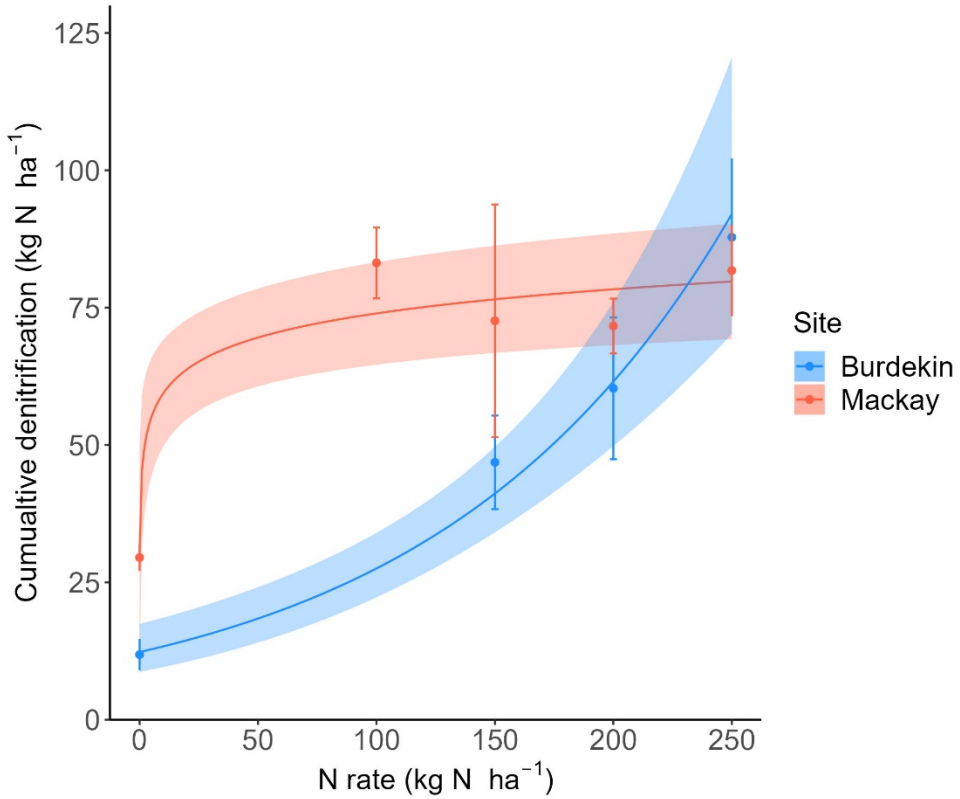

Figure 4 Cumulative denitrification losses over the crop growing season in response to N fertiliser rates at the Burdekin (blue) and Mackay (red) sites. Points and error bars indicate mean values and standard errors. Lines and shaded areas indicate fitted curves and 95% confidence intervals, respectively

3.3 Fertiliser N contribution to denitrification losses (N_2O+N_2)

Contribution of N fertiliser to N_2 emissions was high within 50 DAF, accounting for > 50% and 70% of N_2 emissions at the Burdekin and at the Mackay site, respectively, with a diminishing contribution for the rest of the measurement period (Fig. S1). Of the cumulative N_2 emissions, 51.0–57.5% and 43.1–51.0% were derived from fertiliser N at the Burdekin and Mackay sites, respectively. Cumulative fertiliser-derived N_2O+N_2 emissions ranged from 23.9 to 45.8 and 34.2 to 41.7 kg N ha^{-1} at the Burdekin and Mackay sites, respectively (Fig. 5). Cumulative fertiliser-derived N_2O+N_2 emissions accounted for 30.8–33.3% and 30.5–77.5% of the overall fertiliser ^{15}N loss, at the Burdekin and Mackay sites, respectively (Fig. 5). The percentage of fertiliser N lost as N_2O+N_2 was larger at the Mackay site ($P = 0.02$) and decreased with increasing N rates at both sites ($P = 0.009$). Contribution of fertiliser N to N_2O+N_2 emissions accounted for 15.9–18.3% and 16.7–35.9% of the N applied at the Burdekin and Mackay sites, respectively.

Emissions of N_2O+N_2 derived from soil N in the fertilised treatments were 22.9–42.1 and 35.4–47.3 kg N ha^{-1} at the Burdekin and Mackay sites, respectively.

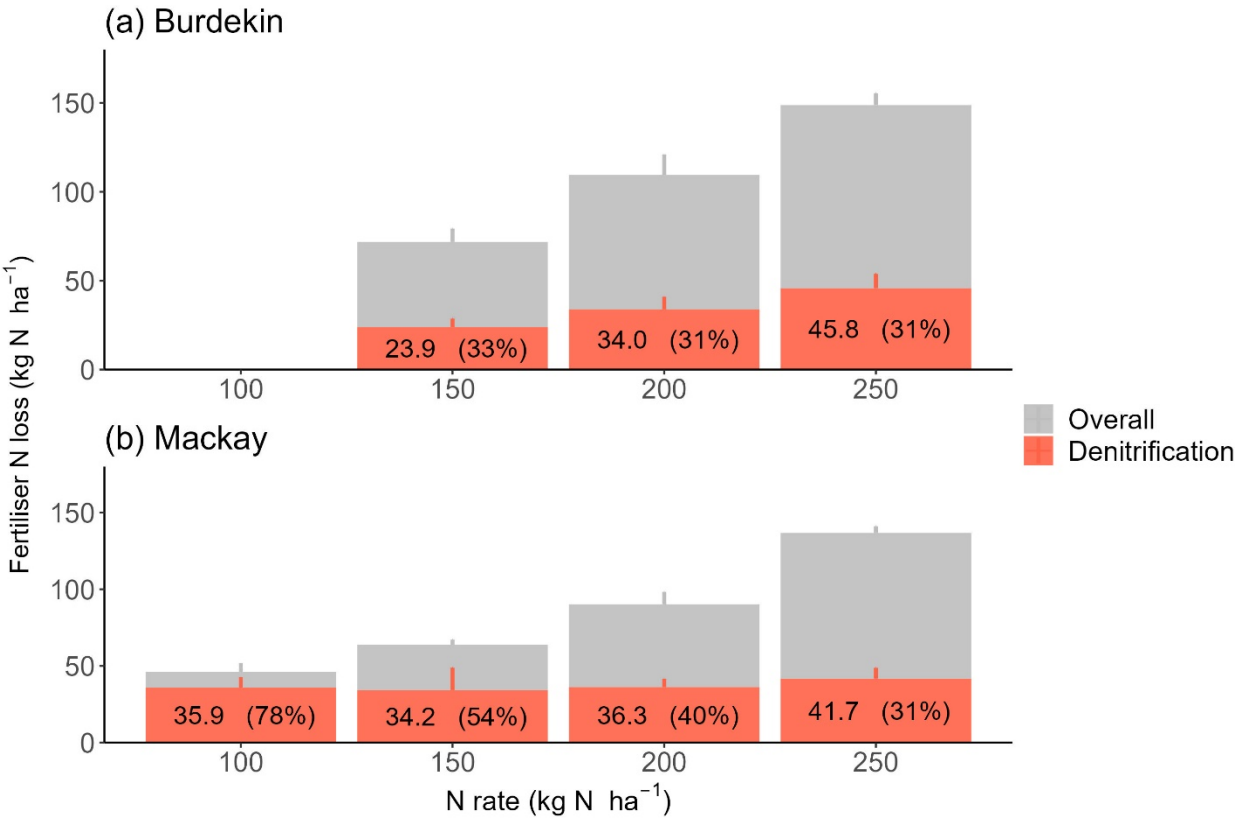

Figure 5 Cumulative fertiliser-derived denitrification losses (red) in comparison to overall fertiliser ^{15}N loss (grey) in response to N fertiliser rates 100, 150, 200 and 250 kg N ha^{-1} at the Burdekin (a) and Mackay (b) sites. Error bars indicate standard errors

4 Discussion

The unique combination of high-frequency N_2O and in-situ $N_2O/(N_2O+N_2)$ ratio (RN_2O) measurements using automated GHG monitoring systems and ^{15}N gas flux method together with GAMMs enabled us to quantify field-scale N_2O and N_2 emissions in response to N fertiliser rates in two sugarcane systems over the whole crop growing season. This method accounts for the dynamic nature of the RN_2O considering the overlapping effects of key drivers of N_2O and N_2 production, delivering robust estimates of N_2 emissions at the field scale. Furthermore, comparing fertiliser-derived N_2O+N_2 emissions to fertiliser ^{15}N loss allowed us to validate the estimated N_2 emissions at the cumulative scale. Applying this method across two intensively managed sugarcane systems showed a) > 80 kg N ha^{-1} lost as N_2O+N_2 over the

growing season, with b) emissions dominated by N_2 accounting for > 95% of N_2O+N_2 losses, and c) that 31-78% of ^{15}N fertiliser losses occurred in the form of N_2O+N_2. The method proposed here can be used as a blueprint approach to deliver seasonal denitrification estimates, targeting a key uncertainty in N budgets of different agroecosystems.

4.1 Estimating N_2 emissions over the crop growing season using RN_2O

Daily The high temporal variability of observed RN_2O ranging from < 0.01 to 0.768 (Fig. 1) emphasises the need to account for dynamic changes in RN_2O to estimate N_2 emissions. The use of GAMMs in this study allowed us to express RN_2O as a function of soil water content, temperature, soil mineral N content and CO_2 emissions, accounting for their effect on the RN_2O at both temporal and spatial scales (Fig. 2). Banding of N fertiliser on or beside the bed creates a distinct zone in and close to the band with high N availability, decreasing towards the furrow. Direct measurements of RN_2O in the unfertilised furrow are not possible with the ^{15}N gas flux method, as it requires the application of ^{15}N fertiliser, highlighting the need for the GAMMs to estimate RN_2O accounting for changes in N availability in the furrow. Higher values of RN_2O as a result of higher N-substrate availability are consistent with the increase in observed RN_2O from the band with increasing N fertiliser rates (Table 2). This relationship is also shown by the higher values of predicted RN_2O from the bed than the furrow at the Mackay site (Table 2), where the application of a single N fertiliser band likely increased spatial differences in N availability as compared to the Burdekin site with banding on both sides of the bed. Differences in RN_2O may be explained by preferential NO_3^- reduction over N_2O in zones of high NO_3^- availability around the fertiliser band (Friedl et al., 2020b; Senbayram et al., 2019). Since banding of N fertiliser is a common practice in intensively managed cropping systems, accounting for its effects on RN_2O as demonstrated here is of therefore of great importance to upscaling N_2 emissions.

It is noteworthy that in contrast to previous studies (Bizimana et al., 2022; Wang et al., 2020), RN_2O data in the study presented here are based on field measurements, which removes the need for measurements of the ratio between N_2O and N_2 using laboratory assays. In-situ measurements avoid a potential bias due to the disturbance of the soil and the absence of plants in the laboratory incubation. An incubation study using the soil samples from the Burdekin site without plants found much lower RN_2O < 0.03 across the whole measurement period compared to this study despite comparable ranges of soil factors (Kirkby et al., personal communication). Both smaller (Bizimana et al., 2022) and larger (Wang et al., 2020) N_2O emissions were reported under laboratory conditions compared to in-situ measurements, indicating an inconsistent discrepancy in RN_2O between field and laboratory measurements. This discrepancy emphasises the need for in-situ measurements as presented here. However, field measurements are likely

to show a higher degree of variability, which was reflected in 52% of deviance explained on average when fitting GAMMs to the observed RN_2O with cross-validation. Fitting GAMMs to the entire dataset without cross-validation resulted in 86% of deviance explained, comparable to the multivariate model of Wang et al. (2020) which explained 92% of the variability of RN_2O. In this study, the cross-validated model by replicate was used to extrapolate at both temporal and spatial scales. Setting the k-fold validation across replicates considerably minimised the potential model overfitting observed when using the entire dataset for model training (Dorich et al., 2020). Comparing the fertiliser-derived N_2O+N_2 with the overall fertiliser ^{15}N loss allowed us to constrain the RN_2O modelling with GAMMs. This constraint at the cumulative scale reduced the uncertainty in N_2 estimates, emphasising the advantage of in-situ N_2O and N_2 measurements with the ^{15}N gas flux method combined with fertiliser ^{15}N recovery measurements.

Applying predicted values of RN_2O to high temporal-resolution N_2O measurements gave estimates of daily N_2 emissions over the season (Fig 3). Similar to N_2O, the majority of N_2 emissions occurred within 100 days after fertilisation, which is consistent with peaks in soil NO_3- availability (Takeda et al., 2021a). High NO_3^- substrate availability for denitrification together with limited O_2 in the soil following intense rainfall and/or irrigation promoted N loss in the form of N_2, which accounted for > 95% of total N_2O+N_2 emissions over the crop growing season (Table 2). On the other hand, the average of observed RN_2O without temporal and spatial upscaling demonstrated up to 9% and 19% of N_2O+N_2 losses as N_2O (Table 2). This discrepancy indicates an underestimation of N_2 emissions if the average of observed RN_2O was directly applied to N_2O emissions. Using fixed RN_2O values from measurements with limited coverage of environmental conditions may therefore lead to a bias in estimated N_2 emissions. In turn, this difference emphasises the importance to include a range of soil conditions covering the spatio-temporal variability observed within a cropping system and season when using the ratio between N_2O and N_2 to upscale N_2 emissions to the field scale.

4.2 Denitrification as a major N loss pathway in intensive sugarcane systems

Total N_2O+N_2 emissions over the season exceeded 80 kg N ha^{-1} at both sites (Fig. 4). Denitrification losses have been regarded as a major portion of N budgets in intensively managed sugarcane systems (Bell et al., 2014) but emissions were only measured from the fertiliser band in short-term trials (Warner et al., 2019; Weier et al., 1996; Weier et al., 1998). The lack of seasonal estimates of denitrification losses in sugarcane hinders the comparison to the range of N_2+N_2O emissions observed in the study presented here. In a simulation study, Thorburn et al. (2017) predicted denitrification losses up to 50 kg N ha^{-1} with N fertiliser rates up to 200 kg N ha^{-1} from Australian sugarcane systems. This range is substantially lower than the N_2+N_2O emissions from both sites. Even though denitrification rates are subject to specific site

and environmental conditions, predictions of denitrification losses in biogeochemical models rely mostly on N_2O data. The lack of N_2 data hinders the validation of overall rates, and changes in N_2O may be caused by a change in denitrification rate and/or RN_2O (Del Grosso et al., 2020). Our estimates of seasonal N_2O+N_2 losses not only provide experimental evidence that denitrification is a major pathway of N loss from intensively managed sugarcane systems, but also the opportunity to test and validate the representation of denitrification in biogeochemical models.

Cumulative N_2O+N_2 losses responded exponentially to N fertiliser rates at the Burdekin site but did not increase across the fertilised treatments at the Mackay site (Fig.4), indicating other factors but N availability limited denitrification at the site. Mackay experienced less rainfall and received less irrigation than the Burdekin site in the critical time window three months after fertilisation. Furthermore, irrigation was applied via overhead sprinklers in Mackay, compared to furrow (flood) irrigation in Burdekin. Considering the sandier soil texture (Table 1) at the Mackay site, the differences in management and rainfall indicate an increased frequency of aerobic conditions in the soil at the Mackay site compared to the Burdekin site (Takeda et al., 2022), limiting the response of denitrification to N rate. Regardless, relatively large N_2O+N_2 losses > 50 kg N ha^{-1} were consistently observed at high N rates above the recommended N rate (≥ 200 kg N ha^{-1}) across the sites (Fig. 4), suggesting increased N substrate availability for N losses via denitrification.

Denitrification was dominated by N_2 emissions (Table 2) and accounted for up to 33% and 78% of the overall fertiliser ^{15}N loss (Fig. 5), showing that a large fraction of N fertiliser loss occurs in the form of environmentally benign N_2. The relative contribution of N_2O+N_2 losses to overall fertiliser ^{15}N loss however decreased with increasing N rates (Fig. 5). This suggests increasing significance of other reactive N loss pathways including ammonia volatilisation, leaching and runoff with increasing N rates, as denitrification may become limited by factors other than N availability. Losses of N_2O+N_2 accounted for a smaller proportion of fertiliser ^{15}N loss at the Burdekin site compared to the Mackay site, which is consistent with furrow irrigation and severe flooding events likely causing greater losses of N fertiliser via leaching and runoff at the Burdekin site. Loss of N via runoff and leaching from Australian sugarcane systems is currently estimated to account for 46–65% of the total dissolved inorganic N load to the Great Barrier Reef (GBR) (Bartley et al., 2017). Increasing N losses via runoff and leaching with increasing N rates have been mostly demonstrated by simulation studies (Reading et al., 2019; Thorburn et al., 2017; Vilas et al., 2022). The study presented here shows that even though a large proportion of N fertiliser loss from sugarcane systems occurs as environmentally benign N_2, more N is lost via environmentally harmful pathways of N loss including ammonia volatilisation, leaching and runoff as N rates increase. These findings suggest that even if N_2O+N_2 losses aren't responding to increasing N rates, environmental costs of sugarcane production are likely to show a non-linear response to N fertiliser.

The large amounts of soil N contributing to N_2O+N_2 across N rates (23–47 kg N ha^{-1}) corroborate the importance of mineralised N for N cycling in sugarcane soils (Takeda et al., 2022). These exports of soil N, together with the plant N uptake derived from soil N (67–122 kg N ha^{-1}), largely exceeded the fertiliser ^{15}N remaining in the soil (40–60 kg N ha^{-1}) across N rates, even when accounting for N in the crop residue which can be returned (~ 60 kg N ha^{-1}). This negative balance demonstrates the ineffectiveness of increasing N fertiliser rates to compensate for soil N depletion. Higher rates of banded N fertiliser application with the aim of carrying surplus N into subsequent seasons ("N-bank" concept) were reported to be associated with high risks of N losses under wet conditions in sub-tropical sorghum systems (Rowlings et al., 2022). The N balance in the study here suggests long-term soil N depletion despite high N inputs in intensively managed sugarcane systems. Together with the non-linear responses of N_2O+N_2 losses and their contribution to fertiliser ^{15}N loss, these results indicate that increasing N fertiliser rates result in lower NUE and higher environmental costs but also don't prevent soil N mining. Maintaining crop productivity while reducing environmental impacts therefore requires N fertiliser rate strategies integrated with additional measures such as the use of enhanced efficiency fertilisers (Connellan & Thompson, 2022) and rotation with legume crops (Otto et al., 2020).

4.3 Extrapolating RN_2O to a wider range of cropping systems towards the global N budget

Denitrification losses have been assumed to account for a significant portion of the global terrestrial N budget despite uncertainties due to limited evaluation at the plot scale (Bouwman et al., 2013; Houlton & Bai, 2009; Scheer et al., 2020). Given that measurements of N_2O emissions are relatively well established and conducted globally, the values of RN_2O play a critical role in estimating the global N budget. Nevertheless, agricultural systems or crop management practices have not been differentiated in most of the reports to date. For example, Scheer et al. (2020) showed a mean RN_2O of 0.11 for agricultural soils and 0.02 for wetlands by summarising the previously reported RN_2O values. The values of RN_2O 0.024–0.058 (Table 2) based on the cumulative N_2 and N_2O emissions in the study presented herein are indicative of intensively managed cropping systems with high N and water inputs. Compared to the range given by Scheer et al. (2020), this would shift denitrification losses from agricultural soils towards the upper end of the current uncertainty range. The method presented in this study provides a unique tool to estimate seasonal denitrification losses accounting for spatial and temporal variability in intensive agroecosystems. This is therefore well suited to generate data that can close the gap in current N budgets, helping to encourage actions to mitigate N pollution.

Refinements of the global N budget require the effects of cropping systems and site conditions on RN_2O to be incorporated. Within this study, the larger RN_2O at the Mackay site (Table 2) may reflect the

effect of the low pH (4.1) compared to the Burdekin site (pH 6.9) (Table 1) shifting the ratio towards N_2O (Dannenmann et al., 2008; Russenes et al., 2016; Šimek & Cooper, 2002). The sandier soil texture may have led to better drainage and larger gas diffusivity at the Mackay site, contributing to the larger RN_2O (Friedl et al., 2017). On the other hand, GCTB management at the Mackay site possibly promoted completion of denitrification and thus reduced RN_2O by preventing evaporation and thus promoting anaerobic conditions (Weier et al., 1993). Accounting for these effects individually to generalise RN_2O estimates requires further data collection across a wide range of environmental conditions such as cropping systems, management practices, soil pH and texture. Controlling environmental factors in laboratory assays can aid in disentangling such overlapping effects, highlighting the need to integrate both laboratory and in-situ measurements of N_2O and N_2 in future research. Generalised estimation of RN_2O covering a wider range of cropping systems and environmental conditions, together with increasing robust in-situ measurements of N_2O emissions, will aid the accuracy of global N budget estimates as well as the identification of hot spots of denitrification losses.

5 Conclusions

This is the first study establishing the response of cumulative denitrification losses (N_2O+N_2) to N fertiliser rates over the whole crop growing season at the plot scale based on in-situ measurements. We propose the integration of in-situ RN_2O with the ^{15}N gas flux method, high-frequency N_2O with an automated GHG monitoring system and fertiliser ^{15}N recovery measurements as a novel and robust method applicable to a wide range of cropping systems to quantify cumulative denitrification losses under field conditions. In contrast to previous approaches, this method accounts for both temporal as well as spatial variability of RN_2O and includes in-situ data for validation of denitrification losses at the cumulative scale. The use of this method demonstrated that seasonal denitrification losses were dominated by N_2 emissions, and accounted for 31–78% of total N fertiliser losses, providing critical evidence for its significance as an N loss pathway from sugarcane systems. The non-linear response of cumulative denitrification losses to increasing N rates, with > 80 kg N ha^{-1} emitted as N_2 and N_2O emphasises the agronomic and environmental inefficiency of excessive N fertiliser application. Even though a large proportion of N fertiliser loss occurred as environmentally benign N_2, more N was lost via environmentally harmful pathways including ammonia volatilisation, leaching and runoff with increasing N rates. These findings highlight that excessive N rates not only increase agronomic inefficiencies, but also the environmental footprint of intensive sugarcane production. This research delivers critical data targeting key uncertainties in biogeochemical models and will aid parameterisation and improvement of denitrification algorithms, advancing our understanding of N cycles across scales. These improvements are urgently needed to develop N fertiliser

rate strategies integrated with soil fertility management and simulate their long-term impacts, to maintain crop productivity while reducing environmental impacts of intensive agroecosystems.

Acknowledgements

The authors have no relevant financial or non-financial interests to disclose. This study was funded by Sugar Research Australia. The authors would like to thank Farmacist and Sheree Biddle for their assistance as well as Richard Kelly and Mario Torrisi for the use of their property as research sites. Some of the data reported in this paper were obtained at the Central Analytical Research Facility operated by the Institute for Future Environments at Queensland University of Technology.

References

Baily, A., Watson, C. J., Laughlin, R., Matthews, D., McGeough, K., & Jordan, P. (2012). Use of the ^{15}N gas flux method to measure the source and level of N_2O and N_2 emissions from grazed grassland. *Nutrient Cycling in Agroecosystems*, *94*, 287-298. https://doi.org/https://doi.org/10.1007/s10705-012-9541-x

Bartley, R., Waters, D., Turner, R., Kroon, F., Wilkinson, S., Garzon-Garcia, A., Kuhnert, P., Lewis, S., Smith, R., Bainbridge, Z., Olley, J., Brooks, A., Burton, J., Brodie, J., & Waterhouse, J. (2017). *Scientific Consensus Statement 2017: A synthesis of the science of land-based water quality impacts on the Great Barrier Reef, Chapter 2: Sources of sediment, nutrients, pesticides and other pollutants to the Great Barrier Reef.* (Scientific Consensus Statement 2017: A synthesis of the science of land-based water quality impacts on the Great Barrier Reef, Issue.

Bates, D., Mächler, M., Bolker, B. M., & Walker, S. C. (2015). Fitting linear mixed-effects models using lme4. *Journal of Statistical Software*, *67*. https://doi.org/https://doi.org/10.18637/jss.v067.i01

Bell, M. J., Biggs, J., McKellar, L. B., Connellan, J., Di Bella, L., Dwyer, R., Empson, M., Garside, A. J., Harvey, T., Kraak, J., Lakshmanan, P., Lamb, D. W., Meier, E., Moody, P., Muster, T., Palmer, J., Robinson, N., Robson, A., Salter, B., . . . Wood, A. (2014). *A review of nitrogen use efficiency in sugarcane*. Sugar Research Australia.

Bizimana, F., Luo, J., Timilsina, A., Dong, W., Gaudel, G., Ding, K., Qin, S., & Hu, C. (2022). Estimating field N_2 emissions based on laboratory-quantified $N_2O/(N_2O + N_2)$ ratios and field-quantified N_2O emissions. *Journal of Soils and Sediments*. https://doi.org/10.1007/s11368-022-03212-0

Bizimana, F., Timilsina, A., Dong, W., Uwamungu, J. Y., Li, X., Wang, Y., Pandey, B., Qin, S., & Hu, C. (2021). Effects of long-term nitrogen fertilization on N_2O, N_2 and their yield-scaled emissions in

a temperate semi-arid agro-ecosystem. *Journal of Soils and Sediments*, *21*(4), 1659-1671. https://doi.org/https://doi.org/10.1007/s11368-021-02903-4

Bouwman, A. F., Beusen, A. H. W., Griffioen, J., Van Groenigen, J. W., Hefting, M. M., Oenema, O., Van Puijenbroek, P. J. T. M., Seitzinger, S., Slomp, C. P., & Stehfest, E. (2013). Global trends and uncertainties in terrestrial denitrification and N_2O emissions. *Philosophical Transactions of the Royal Society B: Biological Sciences*, *368*(1621), 20130112. https://doi.org/https://doi.org/10.1098/rstb.2013.0112

Buchen, C., Lewicka-Szczebak, D., Fuß, R., Helfrich, M., Flessa, H., & Well, R. (2016). Fluxes of N_2 and N_2O and contributing processes in summer after grassland renewal and grassland conversion to maize cropping on a Plaggic Anthrosol and a Histic Gleysol. *Soil Biology and Biochemistry*, *101*, 6-19. https://doi.org/https://doi.org/10.1016/j.soilbio.2016.06.028

Burchill, W., Lanigan, G. J., Li, D., Williams, M., & Humphreys, J. (2016). A system N balance for a pasture-based system of dairy production under moist maritime climatic conditions. *Agriculture, Ecosystems & Environment*, *220*, 202-210. https://doi.org/https://doi.org/10.1016/j.agee.2015.12.022

Butterbach-Bahl, K., Willibald, G., & Papen, H. (2002). Soil core method for direct simultaneous determination of N_2 and N_2O emissions from forest soils. *Plant and Cell Physiology*, *240*, 105-116. https://doi.org/https://doi.org/10.1029/92gb02124

Chen, T., Oenema, O., Li, J., Misselbrook, T., Dong, W., Qin, S., Yuan, H., Li, X., & Hu, C. (2019). Seasonal variations in N_2 and N_2O emissions from a wheat–maize cropping system. *Biology and Fertility of Soils*, *55*, 539-551. https://doi.org/https://doi.org/10.1007/s00374-019-01373-8

Connellan, J., & Thompson, M. (2022). *Support of cane farmer trials of enhanced efficiency fertiliser in the catchments of the Great Barrier Reef: Final report 2016/807*.

Dannenmann, M., Butterbach-Bahl, K., Gasche, R., Willibald, G., & Papen, H. (2008). Dinitrogen emissions and the N_2:N_2O emission ratio of a Rendzic Leptosol as influenced by pH and forest thinning. *Soil Biology and Biochemistry*, *40*(9), 2317-2323. https://doi.org/https://doi.org/10.1016/j.soilbio.2008.05.009

De Rosa, D., Rowlings, D. W., Fulkerson, B., Scheer, C., Friedl, J., Labadz, M., & Grace, P. R. (2020). Field-scale management and environmental drivers of N_2O emissions from pasture-based dairy systems. *Nutrient Cycling in Agroecosystems*, *117*, 299–315. https://doi.org/https://doi.org/10.1007/s10705-020-10069-7

Del Grosso, S. J., Smith, W., Kraus, D., Massad, R. S., Vogeler, I., & Fuchs, K. (2020). Approaches and concepts of modelling denitrification: increased process understanding using observational data

can reduce uncertainties. *Current Opinion in Environmental Sustainability*, *47*, 37-45. https://doi.org/https://doi.org/10.1016/j.cosust.2020.07.003

Dorich, C. D., De Rosa, D., Barton, L., Grace, P., Rowlings, D., Migliorati, M. D. A., Wagner-Riddle, C., Key, C., Wang, D., Fehr, B., & Conant, R. T. (2020). Global Research Alliance N_2O chamber methodology guidelines: Guidelines for gap-filling missing measurements [https://doi.org/10.1002/jeq2.20138]. *Journal of Environmental Quality*, *49*(5), 1186-1202. https://doi.org/https://doi.org/10.1002/jeq2.20138

Friedl, J., Cardenas, L. M., Clough, T. J., Dannenmann, M., Hu, C., & Scheer, C. (2020a). Measuring denitrification and the N_2O:(N_2O+N_2) emission ratio from terrestrial soils. *Current Opinion in Environmental Sustainability*, *47*, 61-71. https://doi.org/https://doi.org/10.1016/j.cosust.2020.08.006

Friedl, J., Scheer, C., Rowlings, D. W., Deltedesco, E., Gorfer, M., De Rosa, D., Grace, P. R., Müller, C., & Keiblinger, K. M. (2020b). Effect of the nitrification inhibitor 3,4-dimethylpyrazole phosphate (DMPP) on N-turnover, the N_2O reductase-gene nosZ and N_2O:N_2 partitioning from agricultural soils. *Scientific Reports*, *10*(1), 2399. https://doi.org/https://doi.org/10.1038/s41598-020-59249-z

Friedl, J., Scheer, C., Rowlings, D. W., McIntosh, H. V., Strazzabosco, A., Warner, D. I., & Grace, P. R. (2016). Denitrification losses from an intensively managed sub-tropical pasture - Impact of soil moisture on the partitioning of N_2 and N_2O emissions. *Soil Biology and Biochemistry*, *92*, 58-66. https://doi.org/https://doi.org/10.1016/j.soilbio.2015.09.016

Friedl, J., Scheer, C., Rowlings, D. W., Mumford, M. T., & Grace, P. R. (2017). The nitrification inhibitor DMPP (3,4-dimethylpyrazole phosphate) reduces N_2 emissions from intensively managed pastures in subtropical Australia. *Soil Biology and Biochemistry*, *108*, 55-64. https://doi.org/https://doi.org/10.1016/j.soilbio.2017.01.016

Grace, P. R., van der Weerden, T. J., Rowlings, D. W., Scheer, C., Brunk, C., Kiese, R., Butterbach-Bahl, K., Rees, R. M., Robertson, G. P., & Skiba, U. M. (2020). Global Research Alliance N_2O chamber methodology guidelines: Considerations for automated flux measurement. *Journal of Environmental Quality*, *49*(5), 1126-1140. https://doi.org/https://doi.org/10.1002/jeq2.20124

Groffman, P. M., Altabet, M. A., Böhlke, J. K., Butterbach-Bahl, K., David, M. B., Firestone, M. K., Giblin, A. E., Kana, T. M., Nielsen, L. P., & Voytek, M. A. (2006). Methods for measuring denitrification: Diverse approaches to a difficult problem. *Ecological Applications*, *16*, 2091-2122. https://doi.org/https://doi.org/10.1890/1051-0761(2006)016[2091:MFMDDA]2.0.CO;2

Henry, S., Texier, S., Hallet, S., Bru, D., Dambreville, C., Chèneby, D., Bizouard, F., Germon, J. C., & Philippot, L. (2008). Disentangling the rhizosphere effect on nitrate reducers and denitrifiers: insight into the role of root exudates [https://doi.org/10.1111/j.1462-2920.2008.01599.x].

Environmental Microbiology, *10*(11), 3082-3092. https://doi.org/https://doi.org/10.1111/j.1462-2920.2008.01599.x

Houlton, B. Z., & Bai, E. (2009). Imprint of denitrifying bacteria on the global terrestrial biosphere. *Proceedings of the National Academy of Sciences*, *106*(51), 21713-21716. https://doi.org/10.1073/pnas.0912111106

IPCC. (2021). *Climate Change 2021: The Physical Science Basis. Contribution of Working Group I to the Sixth Assessment Report of the Intergovernmental Panel on Climate Change*. C. U. Press.

Isbell, R. (2016). *The Australian Soil Classification*. CSIRO publishing.

IUSS Working Group. (2014). *World reference base for soil resources 2014. International soil classification system for naming soils and creating legends for soil maps* (World Soil Resources Report, Issue.

Malique, F., Ke, P., Boettcher, J., Dannenmann, M., & Butterbach-Bahl, K. (2019). Plant and soil effects on denitrification potential in agricultural soils. *Plant and Soil*, 459-474. https://doi.org/10.1007/s11104-019-04038-5

Moritz, S., & Bartz-Beielstein, T. (2017). imputeTS: Time Series Missing Value Imputation in R. *The R Journal*, *9*, 207-218. https://doi.org/https://doi.org/10.32614/rj-2017-009

Mosier, A., & Schimel, D. (1993). Nitrification and denitrification. In *Nitrogen isotope techniques* (pp. 181-208). Elsevier.

Otto, R., Pereira, G. L., Tenelli, S., Carvalho, J. L. N., Lavres, J., de Castro, S. A. Q., Lisboa, I. P., & Sermarini, R. A. (2020). Planting legume cover crop as a strategy to replace synthetic N fertilizer applied for sugarcane production. *Industrial Crops and Products*, *156*, 112853. https://doi.org/https://doi.org/10.1016/j.indcrop.2020.112853

Portmann, R. W., Daniel, J. S., & Ravishankara, A. R. (2012). Stratospheric ozone depletion due to nitrous oxide: Influences of other gases. *Philosophical Transactions of the Royal Society B: Biological Sciences*, *367*, 1256-1264. https://doi.org/https://doi.org/10.1098/rstb.2011.0377

Qin, S., Hu, C., Clough, T. J., Luo, J., Oenema, O., & Zhou, S. (2017). Irrigation of DOC-rich liquid promotes potential denitrification rate and decreases $N_2O/(N_2O+N_2)$ product ratio in a 0–2 m soil profile. *Soil Biology and Biochemistry*, *106*, 1-8. https://doi.org/https://doi.org/10.1016/j.soilbio.2016.12.001

R Core Team. (2018). *R: A language and environment for statistical computing. R Foundation for Statistical Computing*. In https://www.R-project.org/

Ravishankara, A. R., Daniel, J. S., & Portmann, R. W. (2009). Nitrous Oxide (N_2O): The Dominant Ozone-Depleting Substance Emitted in the 21st Century. *Science*, *326*(5949), 123. https://doi.org/https://doi.org/10.1126/science.1176985

Reading, L. P., Bajracharya, K., & Wang, J. (2019). Simulating deep drainage and nitrate leaching on a regional scale: implications for groundwater management in an intensively irrigated area. *Irrigation Science*, *37*, 561-581. https://doi.org/https://doi.org/10.1007/s00271-019-00636-4

Rowlings, D. W., Lester, D. W., Grace, P. R., Scheer, C., De Rosa, D., De Antoni Migliorati, M., Friedl, J., & Bell, M. J. (2022). Seasonal rainfall distribution drives nitrogen use efficiency and losses in dryland summer sorghum. *Field Crops Research*, *283*, 108527. https://doi.org/https://doi.org/10.1016/j.fcr.2022.108527

Rowlings, D. W., Scheer, C., Liu, S., & Grace, P. R. (2016). Annual nitrogen dynamics and urea fertilizer recoveries from a dairy pasture using ^{15}N; effect of nitrification inhibitor DMPP and reduced application rates. *Agriculture, Ecosystems & Environment*, *216*, 216-225. https://doi.org/https://doi.org/10.1016/j.agee.2015.09.025

Russenes, A. L., Korsaeth, A., Bakken, L. R., & Dörsch, P. (2016). Spatial variation in soil pH controls off-season N_2O emission in an agricultural soil. *Soil Biology and Biochemistry*, *99*, 36-46. https://doi.org/https://doi.org/10.1016/j.soilbio.2016.04.019

Scheer, C., Fuchs, K., Pelster, D. E., & Butterbach-Bahl, K. (2020). Estimating global terrestrial denitrification from measured N_2O:($N_2O + N_2$) product ratios. *Current Opinion in Environmental Sustainability*, *47*, 72-80. https://doi.org/https://doi.org/10.1016/j.cosust.2020.07.005

Scheer, C., Wassmann, R., Butterbach-Bahl, K., Lamers, J. P. A., & Martius, C. (2009). The relationship between N_2O, NO, and N_2 fluxes from fertilized and irrigated dryland soils of the Aral Sea Basin, Uzbekistan. *Plant and Soil*, *314*, 273-283. https://doi.org/https://doi.org/10.1007/s11104-008-9728-8

Scholefield, D., Hawkins, J., & Jackson, S. (1997). Development of a helium atmosphere soil incubation technique for direct measurement of nitrous oxide and dinitrogen fluxes during denitrification. *Soil Biology and Biochemistry*, *29*(9-10), 1345-1352. https://doi.org/https://doi.org/10.1016/S0038-0717(97)00021-7

Schroeder, B. L., Hurney, A. P., Wood, A. W., Moody, P. W., & Allsopp, P. G. (2010). Concepts and value of the nitrogen guidelines contained in the Australian sugar industry's 'Six Easy Steps' nutrient management program. Proceedings of the International Society of Sugar Cane Technologists,

Schwenke, G., & Haigh, B. (2016). The interaction of seasonal rainfall and nitrogen fertiliser rate on soil N_2O emission, total N loss and crop yield of dryland sorghum and sunflower grown on sub-tropical Vertosols. *Soil Research*, *54*(5), 604-618. https://doi.org/https://doi.org/10.1071/SR15286

Senbayram, M., Budai, A., Bol, R., Chadwick, D., Marton, L., Gündogan, R., & Wu, D. (2019). Soil NO_3^- level and O_2 availability are key factors in controlling N_2O reduction to N_2 following long-

term liming of an acidic sandy soil. *Soil Biology and Biochemistry*, *132*, 165-173. https://doi.org/https://doi.org/10.1016/j.soilbio.2019.02.009

Shcherbak, I., Millar, N., & Robertson, G. P. (2014). Global metaanalysis of the nonlinear response of soil nitrous oxide (N_2O) emissions to fertilizer nitrogen. *Proceedings of the National Academy of Sciences*, *111*, 9199-9204. https://doi.org/https://doi.org/10.1073/pnas.1322434111

Šimek, M., & Cooper, J. E. (2002). The influence of soil pH on denitrification: Progress towards the understanding of this interaction over the last 50 years. *European Journal of Soil Science*, *53*, 345-354. https://doi.org/https://doi.org/10.1046/j.1365-2389.2002.00461.x

Spott, O., Russow, R., Apelt, B., & Stange, C. F. (2006). A ^{15}N-aided artificial atmosphere gas flow technique for online determination of soil N_2 release using the zeolite Köstrolith SX6® [https://doi.org/10.1002/rcm.2722]. *Rapid Communications in Mass Spectrometry*, *20*(22), 3267-3274. https://doi.org/https://doi.org/10.1002/rcm.2722

Takeda, N., Friedl, J., Kirkby, R., Rowlings, D., De Rosa, D., Scheer, C., & Grace, P. (2022). Interaction between soil and fertiliser nitrogen drives plant nitrogen uptake and nitrous oxide (N_2O) emissions in tropical sugarcane systems. *Plant and Soil*. https://doi.org/https://doi.org/10.1007/s11104-022-05458-6

Takeda, N., Friedl, J., Rowlings, D., De Rosa, D., Scheer, C., & Grace, P. (2021a). Exponential response of nitrous oxide (N_2O) emissions to increasing nitrogen fertiliser rates in a tropical sugarcane cropping system. *Agriculture, Ecosystems & Environment*, *313*, 107376. https://doi.org/https://doi.org/10.1016/j.agee.2021.107376

Takeda, N., Friedl, J., Rowlings, D., De Rosa, D., Scheer, C., & Grace, P. (2021b). No sugar yield gains but larger fertiliser ^{15}N loss with increasing N rates in an intensive sugarcane system. *Nutrient Cycling in Agroecosystems*, *121*(1), 99-113. https://doi.org/https://doi.org/10.1007/s10705-021-10167-0

Thorburn, P. J., Biggs, J. S., Palmer, J., Meier, E. A., Verburg, K., & Skocaj, D. M. (2017). Prioritizing Crop Management to Increase Nitrogen Use Efficiency in Australian Sugarcane Crops. *Frontiers in Plant Science*, *8*, 1-16. https://doi.org/https://doi.org/10.3389/fpls.2017.01504

Vilas, M. P., Shaw, M., Rohde, K., Power, B., Donaldson, S., Foley, J., & Silburn, M. (2022). Ten years of monitoring dissolved inorganic nitrogen in runoff from sugarcane informs development of a modelling algorithm to prioritise organic and inorganic nutrient management. *Science of The Total Environment*, *803*, 150019. https://doi.org/https://doi.org/10.1016/j.scitotenv.2021.150019

Wang, R., Pan, Z., Zheng, X., Ju, X., Yao, Z., Butterbach-Bahl, K., Zhang, C., Wei, H., & Huang, B. (2020). Using field-measured soil N_2O fluxes and laboratory scale parameterization of

$N_2O/(N_2O+N_2)$ ratios to quantify field-scale soil N_2 emissions. *Soil Biology and Biochemistry*, *148*, 107904. https://doi.org/https://doi.org/10.1016/j.soilbio.2020.107904

Warner, D. I., Scheer, C., Friedl, J., Rowlings, D. W., Brunk, C., & Grace, P. R. (2019). Mobile continuous-flow isotope-ratio mass spectrometer system for automated measurements of N_2 and N_2O fluxes in fertilized cropping systems. *Scientific Reports*, *9*, 11097. https://doi.org/https://doi.org/10.1038/s41598-019-47451-7

Weier, K., McEwan, C., Vallis, I., Catchpoole, V., & Myers, R. J. A. J. o. A. R. (1996). Potential for biological denitrification of fertilizer nitrogen in sugarcane soils. *47*(1), 67-79.

Weier, K., Rolston, D., & Thorburn, P. J. (1998). The potential of N losses via denitrification beneath a green cane trash blanket. Proceedings of the Australian Society of Sugar Cane Technologists,

Weier, K. L., Doran, J. W., Power, J. F., & Walters, D. T. (1993). Denitrification and the Dinitrogen/Nitrous Oxide Ratio as Affected by Soil Water, Available Carbon, and Nitrate. *Soil Science Society of America Journal*, *57*, 66-72. https://doi.org/https://doi.org/10.2136/sssaj1993.03615995005700010013x

Wood, S. N. (2011). Fast stable restricted maximum likelihood and marginal likelihood estimation of semiparametric generalized linear models. *Journal of the Royal Statistical Society. Series B: Statistical Methodology*, *73*(1), 3-36. https://doi.org/https://doi.org/10.1111/j.1467-9868.2010.00749.x

Zistl-Schlingmann, M., Feng, J., Kiese, R., Stephan, R., Zuazo, P., Willibald, G., Wang, C., Butterbach-Bahl, K., & Dannenmann, M. (2019). Dinitrogen emissions: an overlooked key component of the N balance of montane grasslands. *Biogeochemistry*, *143*(1), 15-30. https://doi.org/https://doi.org/10.1007/s10533-019-00547-8

Global Biogeochemical Cycles

Supporting Information for

Denitrification losses in response to N fertiliser rates – a synthesis of high temporal resolution N_2O, in-situ $^{15}N_2O$ and $^{15}N_2$ measurements and fertiliser ^{15}N recoveries in intensive sugarcane systems

Naoya Takeda*[1], Johannes Friedl*[1], Robert Kirkby[1], David Rowlings[1], Clemens Scheer[1, 2], Daniele De Rosa[3], Peter Grace[1]

[1] Centre for Agriculture and the Bioeconomy, Queensland University of Technology, Brisbane, Queensland, Australia

[2] IMK-IFU, Karlsruhe Institute of Technology, Garmisch-Partenkirchen, Germany

[3] European Commission, Joint Research Centre (JRC), Sustainable Resources Directorate, Land Resources Unit, I-21027 Ispra, Italy

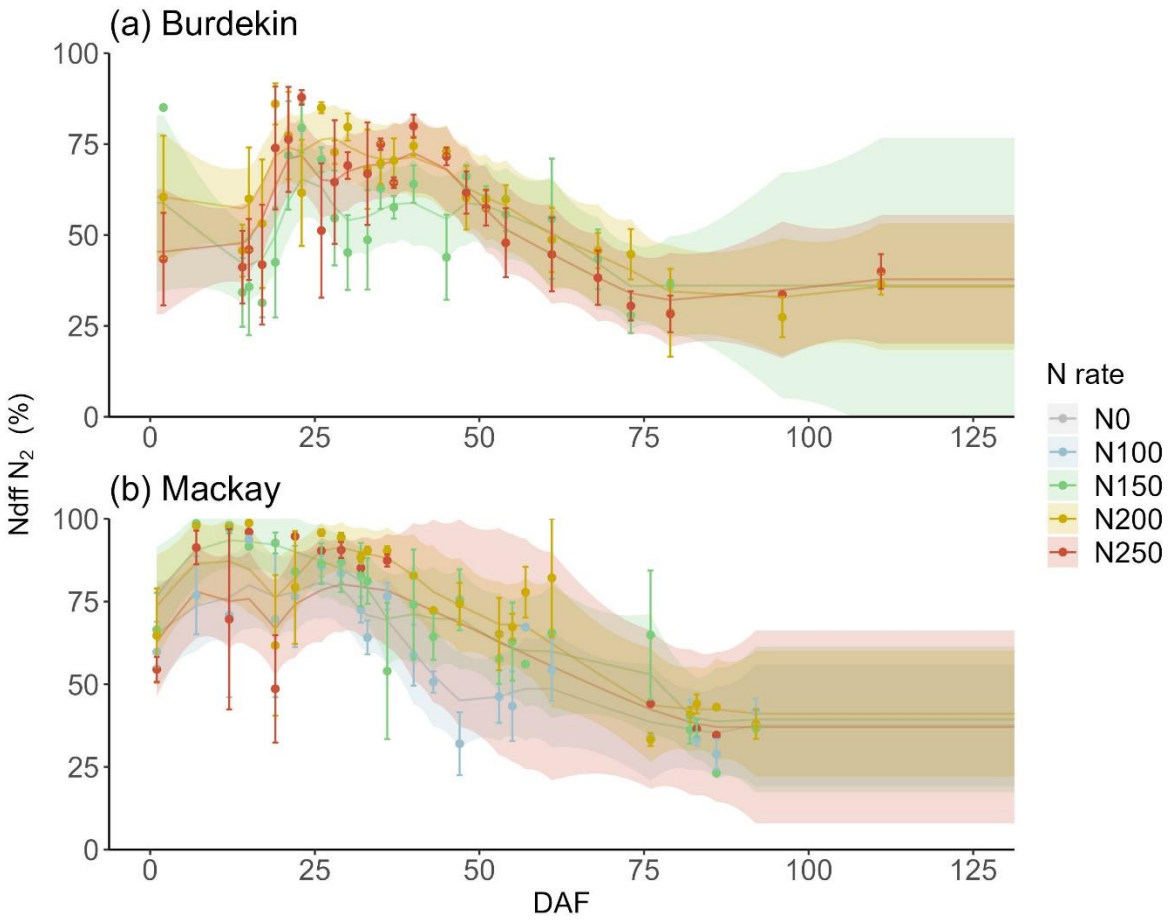

Figure S1 Relative contribution of fertiliser N to N_2 emissions (Ndff N_2) on the fertiliser band over the measurement period across N rates 100, 150, 200 and 250 kg N ha^{-1} at the Burdekin (a) and Mackay (b) sites. Points and error bars indicate mean values and standard errors. Lines and shaded areas indicate fitted curves and 95% confidence intervals

Global Biogeochemical Cycles

Supporting Information for

Denitrification losses in response to N fertiliser rates – a synthesis of high temporal resolution N_2O, in-situ $^{15}N_2O$ and $^{15}N_2$ measurements and fertiliser ^{15}N recoveries in intensive sugarcane systems

Naoya Takeda*[1], Johannes Friedl*[1], Robert Kirkby[1], David Rowlings[1], Clemens Scheer[1, 2], Daniele De Rosa[3], Peter Grace[1]

[1] Centre for Agriculture and the Bioeconomy, Queensland University of Technology, Brisbane, Queensland, Australia

[2] IMK-IFU, Karlsruhe Institute of Technology, Garmisch-Partenkirchen, Germany

[3] European Commission, Joint Research Centre (JRC), Sustainable Resources Directorate, Land Resources Unit, I-21027 Ispra, Italy

S1 Materials and methods

S1.1. Automated chamber system

Acrylic static chambers (0.5 m × 0.5 m × 0.15 m) were mounted on stainless steel frames inserted 10 cm into the soil. The lids of the chambers were opened and closed automatically with pneumatic pistons, and four chambers were closed at one time. Air samples were taken sequentially from each closed chamber, followed by a single-point known standard (Air Liquide, Dallas, TX, USA) of 0.5 ppm N_2O and 800 ppm CO_2 for calibration and drift correction (i.e., after every fourth sample). Changes in headspace N_2O and CO_2 concentration after chamber closure were measured with a gas chromatograph (SRI 8610C, SRI Instruments, Inc., Las Vegas, NV, USA) equipped with a ^{63}Ni electron capture detector (ECD) for N_2O analysis while an infrared gas analyser (LI-820, LI-COR Biosciences, Lincoln, NE, USA) was used for measurements of CO_2. In total, each chamber was sampled four times (every 15 min) over 60 min. This enabled up to eight single flux rates to be determined per chamber and day. The detection limit of the system was 2.0 µg N_2O-N m^{-2} h^{-1} for N_2O. Hourly N_2O and CO_2 fluxes were calculated from the slope of the linear change in gas concentration during the closure period (60 min) and corrected for air temperature, atmospheric

pressure and the ratio of chamber volume to surface area as described in detail by Grace et al. (2020). The coefficient of determination (R^2) for the linear regression was calculated and used as a quality check for the measurement. Flux rates were discarded if R^2 was < 0.80.

S1.2. Manual chamber system

Manual gas sampling was conducted with sealed polyethylene chambers (0.5 m × 0.5 m × 0.15 m). Headspace gas samples were taken between 0900 and 1200 H analogous to the sampling regime of the GHG system, connecting a syringe to a 2-way luer-lock tap installed in the lid of the chamber. Gas samples were injected into pre-evacuated 12 mL glass vials with a double wadded Teflon/silicone septa cap (Labco Exetainer ®, UK) and analysed for N_2O and CO_2 using a Shimadzu GC-2014 Gas Chromatograph (Shimadzu, Kyoto, Japan) at the Central Analytical Research Facility of the Queensland University of Technology, Australia.

S1.3. Gas sampling procedure in the micro plots

Gas samples were taken 1–3 times a week between 0900-1200H with higher frequency after N fertiliser application and irrigation or rainfall events. At the Burdekin site, polyethylene chambers with a headspace height of 19.93 cm were placed on the steel frames, ensuring airtight conditions. Headspace gas samples (20 ml) were taken by connecting a syringe to a 2-way luer-lock tap installed in the lid of the chamber. Gas samples were then injected into a pre-evacuated 12 ml glass vial with a double wadded Teflon/silicone septa cap (Labco, UK). Headspace gas samples were collected at 0, 60 and 180 min after closure. At the Mackay site, airtight polyethylene chambers with a headspace height of 15 cm were placed on the base and connected to a battery-powered sampling unit. The chambers were automatically closed at sampling events according to the pre-programmed schedule and gas samples were collected at 0, 60 and 180 min after the chamber closure. Headspace gas samples (20 ml) were automatically taken and injected into the pre-evacuated 12 ml glass vials sequentially installed on a belt in the sampling unit.

S1.4. The ^{15}N gas flux method

The ^{15}N enrichment of the NO_3^- pool undergoing denitrification (a_p N_2 and a_p N_2O) and the fraction of N_2 and N_2O emitted from this pool (f_p) were calculated following the equations given by Spott et al. (2006)

$$f_p = \frac{a_m - a_{bgd}}{a_p - a_{bgd}} \quad [S1]$$

where a_{bgd} is the ^{15}N abundance of the atmospheric background and a_m is the measured ^{15}N abundance of N_2 from headspace gas samples taken 0 and 180 minutes after closure, respectively. Both a_{bgd} and a_m are calculated as

$$a_i = \frac{{}^{29}R + 2 * {}^{30}R}{2 * (1 + {}^{29}R + {}^{30}R)} \quad [S2]$$

and ${}^{30}x_m$ is the measured fraction of m/z 30 in N_2:

$${}^{30}x_m = \frac{{}^{30}R}{(1 + {}^{29}R + {}^{30}R)} \quad [S3]$$

If only ^{29}R was > the detection limit (DL), f_p was calculated as

$$f_p = \frac{1}{1 - \frac{{}^{29}R(1 - a_p)^2 - 2a_p(1 - a_p)}{{}^{29}R(1 - a_{bgd})^2 - 2a_{bgd}(1 - a_{bgd})}} \quad [S4]$$

using a_p N_2O assuming that N_2 and N_2O were derived from the same NO_3^- pool undergoing denitrification.

S1.5. Plant and soil sampling

All the sugarcane plants in the 2.0 m section were sampled by cutting at ground level and the trash on the ground in the section was also collected, followed by fresh weight measurements. Roughly six stalks from the middle of the 2.0 m section were chosen and separated into tops (above 7th node), stalk and dead leaves. Two green leaves at the 3rd node (L+3) were sampled from the plants from the 2-m section (L3_CR) and the adjacent row (L3_AR) to estimate the fertiliser ^{15}N recovery in the plant in the adjacent rows. After sampling aboveground biomass, remaining stools and major roots were sampled from a 0.5 × 0.5 m square in the middle of the 2.0 m section by digging down to 0.15 m depth. Roots were washed to remove the attached soil and separated into stool and roots. The tops, stalks, dead leaves and trash samples were coarsely ground, subsampled (about 10% on a fresh weight basis) and weighed to calculate partitioning ratios. The plant subsamples, L+3 samples, root samples and stool samples were oven-dried at 60 °C and dry weights were recorded. The stalk samples were further dried with a vacuum oven at 40 °C for 48 hours before fine grinding to avoid aggregation due to sugar.

Soil samples were taken at three to four points between the bed and furrow centres using a soil corer and a post-hole driver down to 1.0 m. At the Burdekin site, the sampling points were 0, 0.25, 0.50, 0.75 m away from the bed centre. At the Mackay site, those were 0, 0.12, 0.40, 0.80 m away from the bed centre in 100N and 250N and the three points except for 0.12 m away from the bed centre in 150N and 200N. Each soil core sample of 1.0 m was separated into 0–0.2, 0.2–0.4, 0.4–0.7, 0.7–1.0 m soil depths and subsamples (about 100 g) were taken.

S1.6. ^{15}N calculation in plant and soil

The percentage of N in the individual plant, soil, N_2O and N_2 samples ('sinks') derived from ^{15}N-labelled fertiliser was calculated from

$$Ndff\ (\%) = \frac{\%^{15}N\ excess\ of\ sink}{\%^{15}N\ excess\ of\ fertiliser} \times 100 \quad [S5]$$

where the $\%^{15}N$ excess used for all sources and sinks was the ^{15}N abundance less an adjustment of $\%^{15}N$ measured for the corresponding plant and soil samples in the 0N plots for background enrichment or the natural abundance (0.0036765) for N_2O and N_2 samples.

Fertiliser N recovered in each plant part (*PlantFN*$_i$) was calculated from

$$PlantFN_i = Biomass_i \times N\ content_i \times \frac{Ndff_i}{100} \quad [S6]$$

where i indicates the plant part. Fertiliser N recovered in tops, stalk, dead leaves and trash were summed to calculate the fertiliser N recovered in the aboveground biomass (*PlantFN*$_{AG}$) in the centre row in each plot. Fertiliser N recovered in the belowground biomass (*PlantFN*$_{BG}$) in the centre row was calculated by summing the fertiliser N recovered in stool and roots. Fertiliser N recovered in the adjacent rows (*PlantFN*$_{AR}$) was calculated in each plot by multiplying the total N uptake in the centre row and the Ndff calculated from L3_AR sample. Fertiliser ^{15}N uptake was then calculated as follows:

$$Fertiliser\ \ ^{15}N\ uptake = (PlantFN_{AG} + PlantFN_{BG} + PlantFN_{AR} \times 2) \quad [S7]$$

To calculate fertiliser ^{15}N recovery in the soil, the distribution of ^{15}N fertiliser across the soil profile between bed and furrow was first analysed to account for the spatial variation caused by banding N fertiliser, following Takeda et al. (2021). (i) Fertiliser N recovered in the soil (*SoilFN*$_{ij}$) of each sample (four points from the bed centre and four depths down to 1.0 m per plot at the centre of the soil layer as the average) was calculated from

$$SoilFN_{ij} = BD_{ij} \times N\ content_{ij} \times \frac{Ndff_{ij}}{100} \quad [S8]$$

where i and j indicate the sampling point and depth per plot. At the Mackay site, the missing *SoilFN*$_{ij}$ values at the sampling point 0.12 m away from the bed centre in 150N and 200N treatments were substituted with the estimated values from regressions by N rates at each soil depth. (ii) The fertiliser ^{15}N recovered in the soil (*SoilFN*$_{ij}$) was then interpolated across one side of the sugarcane row (0.75 m width, x-axis) and down to a soil depth of 1.0 m (y-axis) for each plot by fitting a thin-plate spline using a package "mgcv" (Wood, 2011). (iii) The interpolated fertiliser N recovered in the soil

($SoilFN_{xy}$) was integrated and divided by the area of one side of the row (*Area*, 0.75 m^2) to express fertiliser N recovered in kg N ha^{-1}. Fertiliser ^{15}N recovery in the soil as a proportion to the N rate was then calculated as follows:

$$Fertiliser \quad {}^{15}N\ recovery\ in\ the\ soil\ = \frac{\sum SoilFN_{xy}}{Area} \qquad [S9]$$

Overall fertiliser ^{15}N loss was calculated by the difference between the N applied and fertiliser ^{15}N recovered in the soil and plant.

Calculations for fertiliser ^{15}N recovered in N_2O emissions are detailed in Takeda et al. (2022) and those for N_2 emissions followed the same procedure. Briefly, the proportion of N_2 emissions derived from fertiliser (*Ndff* N_2) at the fertiliser band was first calculated by Equation [S5]. Then, *Ndff* N_2 was gap-filled per N rate over the crop growing season on a daily basis at each site, which were then applied to daily N_2 emissions per plot in the main plots to calculate fertiliser-derived N_2 as follows:

$$Fertiliser\ derived\ N_2\ emissions_{i,j} = N_2\ emissions_{i,j} \times \frac{Ndff\ N_{2i,j}}{100} \qquad [S10]$$

where i and j indicate days after fertilisation and chamber position (i.e. bed or furrow). At the Burdekin site, *Ndff* N_2 at the fertiliser band in micro plots was used for both bed and furrow chambers because both chambers covered the fertiliser band. At the Mackay site, *Ndff* N_2 at the furrow was assumed to be zero because the furrow chamber did not cover the fertiliser band. Contribution of fertiliser N to N_2 was calculated by area-weighted sum of fertiliser-derived N_2 emissions over the crop growing season.

S1.7. Use of generalised additive mixed models

The use of generalised additive mixed models (GAMMs) can quantify non-linear relationships without specifying the functional forms and GAMMs further allow repeated measurements. The distribution of RN_2O and *Ndff* N_2 was assumed Beta distributed, which is suitable to fit variables taking values between 0 and 1, and the logit function was specified as the link function, respectively. A dispersion parameter can further be specified in Beta regressions, which was useful to fit the RN_2O densely distributed near zero. The dispersion parameter was set at 23 based on a comparison of AIC.

To model RN_2O, the site factor was specified as a linear term and the CO_2 emissions measured in the micro plots, soil NH_4^+ and NO_3^- contents measured near the band in the main plots and WFPS and soil temperature measured across the paddock were specified as smooth terms

and the micro plots as the random variable. For RN_2O modelling, cross-validation was performed by splitting datasets into training and testing by replicates (k = 4) and the predictive performance was evaluated by the averaged deviance explained and root mean square error (RMSE). The average of RN_2O predicted across k for each plot and bed/furrow position was used to calculate N_2 emissions.

In gap-filling of *Ndff* N_2, days after fertilisation (DAF) and N rates were specified as the explanatory variables in a tensor product, allowing the changes in *Ndff* N_2 over time to differ between N rate treatments. To account for the repeated measurements of *Ndff* N_2 at the same chamber, 'chamber' was specified as the random variable nested in DAF. The estimated *Ndff* N_2 was then multiplied by 100 to show in percentage.